Application of the Discontinuous Galerkin Method to Supernova Hydrodynamics in `thornado`

Jesse Buffaloe[1], Brandon Barker[2], David Pochik[1], Samuel J. Dunham[4,1], Eirik Endeve[3,1]

[1] The University of Tennessee, Knoxville, [2]Michigan State University, [3]Oak Ridge National Laboratory, [4]Vanderbilt University

The Core-Collapse Supernova Problem

- Massive stars end their lives in a cataclysmic fashion.
- Models tell us a few things[1]:
  - Fusion stops. Gravity compresses core.
  - Compression stops. Bounce produces shock.
  - Shock stalls. Revival by neutrino heating and multi-dimensional hydrodynamics.
  - Process produces gravitational and neutrino radiation, along with heavy elements.

This is a multi-dimensional, multi-physics (e.g., general relativity, hydrodynamics, neutrino transport, nuclear structure) problem.

Want a multi-dimensional numerical method that can be made high-order accurate while faithfully capturing discontinuities.

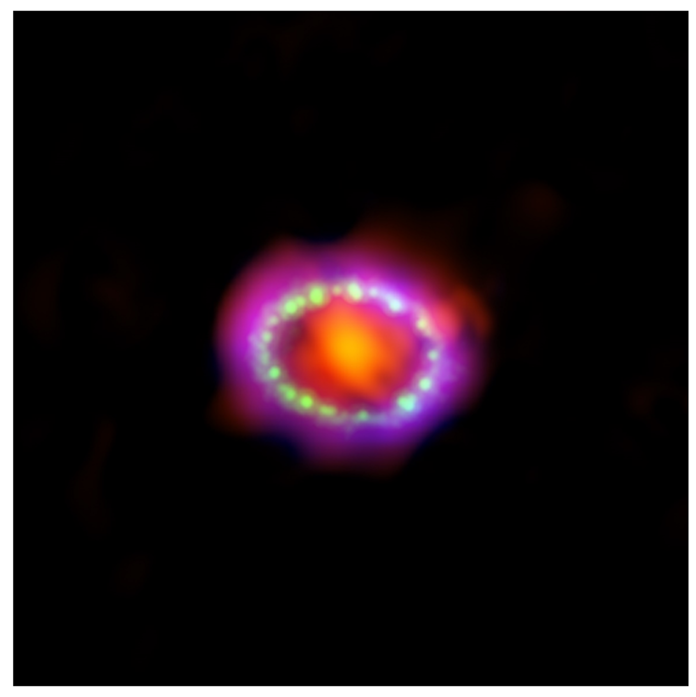

Recent (2017) composite image of Supernova 1987A remnant. (Credit: X-ray: NASA/CXC/SAO/PSU/D. Burrows et al.; Optical: NASA/STScI; Millimeter: NRAO/AUI/NSF)

Standing Accretion Shock Instability (SASI):

- Spherical standing shock (initially at r = 1) between infalling supersonic and subsonic matter.
- Unstable to non-radial perturbations, e.g., $l = 1$ mode.
- The SASI may play a crucial role in supernova dynamics, shock revival, and observables[5].
- 1D results show expected return to stability[5], but 2D shows instability to both $l = 1$ *and* $l = 0$ perturbations (possibly due to non-radial numerical perturbations).

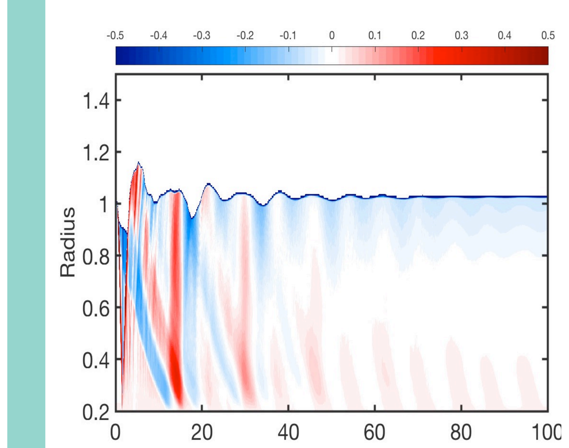

1D radial perturbation test with 256 elements. Perturbation is a shell from r = [1.4 ,1.6] of 3 times the ambient density. Color indicates relative deviation in pressure below the shock radius.[4]

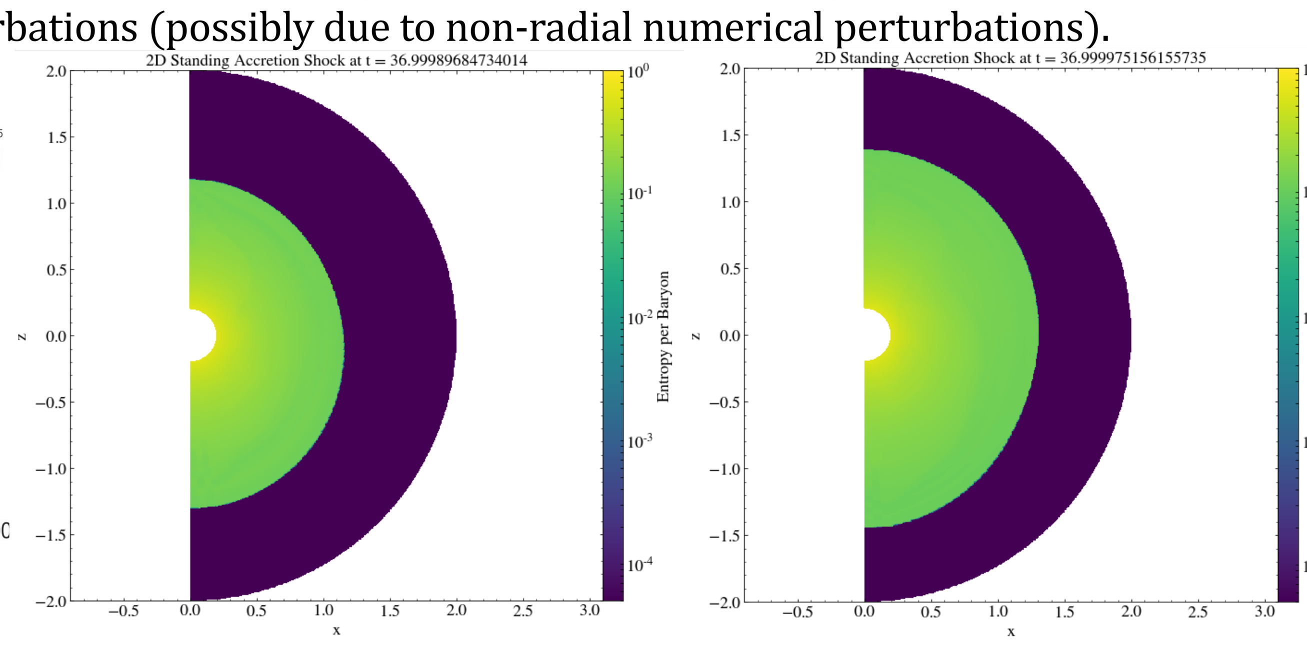

2D $l = 0$ (left) and $l = 1$ (right) perturbation tests with 512 x 64 elements, three nodes per element, characteristic limiting, HLLC flux and 3rd order SSP-RK timestepping. Perturbation is a shell from r = [1.4 ,1.6] of 1.2 times the ambient density.

The Euler Equations

$$\frac{\partial \mathbf{U}}{\partial t} + \frac{1}{\sqrt{\gamma}} \sum_{i=1}^{3} \frac{\partial}{\partial x^i}\left(\sqrt{\gamma}\, \mathbf{F}^i(\mathbf{U})\right) = \mathbf{S}(\mathbf{U})$$

Conserved Variables: $\mathbf{U} = \left(\rho, \rho u_j, E, \rho Y_e\right)^T$

Fluxes: $\mathbf{F}^i(\mathbf{U}) = \left(\rho u^i, \Pi^i_{\ j}, (E+P)u^i, \rho Y_e u^i\right)^T$

Sources: $\mathbf{S}(\mathbf{U}) = \left(0,\ \frac{1}{2}\Pi^{ik}\partial_j \gamma_{ik} - \rho \partial_j \Phi,\ -\rho u^i \partial_i \Phi, 0\right)^T$

- γ_{ij} is a spatial metric with, e.g., $\gamma_{ij} = \mathrm{diag}(1,\ r^2, r^2\sin^2(\theta))$ for spherical polar coordinates.
- Closure is provided by an equation of state (EoS) that is either ideal: $P = (\Gamma - 1)e$, or tabulated: $P = P(\rho, T, Y_e)$.
- For an ideal EoS, ignore evolution of the electron mass density.

The Discontinuous Galerkin (DG) Method

In 1D, our DG method is[4]:

1. Divide the computational domain into elements with nodes at the Legendre-Gauss quadrature points.
2. Minimize the residual for a solution $\mathbf{U_h}$ on cell $\mathbf{K}$ with respect to a set of polynomials $v \in V^k$:

$$\partial_t \int_{\mathbf{K}} \sqrt{\gamma}\, \mathbf{U_h}\, v\, dx + \sqrt{\gamma}\, \hat{\mathbf{F}}(\mathbf{U_h}) v\Big|_{x_H} - \sqrt{\gamma}\, \hat{\mathbf{F}}(\mathbf{U_h}) v\Big|_{x_L} - \int_{\mathbf{K}} \sqrt{\gamma}\, \mathbf{F}(\mathbf{U_h})\, \partial_x v\, dx = \int_{\mathbf{K}} \sqrt{\gamma}\, \mathbf{S}(\mathbf{U_h}) v\, dx$$

3. Use a numerical flux scheme for $\hat{\mathbf{F}}(\mathbf{U_h})$ (HLL or HLLC).
4. Expand $\mathbf{U_h}$ by a sum of Lagrange polynomials on the nodes.
5. Use Legendre-Gauss quadrature to evaluate integrals.
6. Evolve in time using a strong stability-preserving Runge-Kutta method (SSP-RK).

The DG Method: Characteristic Limiting

$$\frac{\partial \mathbf{U}}{\partial t} + \frac{\partial \mathbf{F}(\mathbf{U})}{\partial \mathbf{U}} \frac{\partial \mathbf{U}}{\partial x} = 0$$

Hyperbolic PDE

$$\frac{\partial \mathbf{F}(\mathbf{U})}{\partial \mathbf{U}} = R \Lambda R^{-1}$$

Multiply by R^{-1}

Let $\mathbf{w} = R^{-1}\mathbf{U}$

$$\frac{\partial \mathbf{w}}{\partial t} + \Lambda \frac{\partial \mathbf{w}}{\partial x} = 0$$

Limit Slopes of $\mathbf{w}$

- More effective than limiting on $\mathbf{U}$.
- Extendable to nuclear EoS[7].

The DG Method: Positivity Limiting

- Limit to ensure physicality of solutions.
- Physical domain with nuclear EoS is not globally convex. Ideal EoS methods not applicable.[2]
- For a tabulated EoS, need values within the boundaries of the table (G is the set of allowed states).
- If initial conditions in convex hull of G, then new $\mathbf{U}_K$ is in convex hull of G.[2] If $\mathbf{U_p} \not\subset$ G, then limit toward $\mathbf{U}_K$, with severity determined by a factor θ.[2]
- For specific internal energy, the appropriate limiting factor is found using bisection:

$$\epsilon\left(\theta \mathbf{U_p} + (1-\theta)\mathbf{U_K}\right) - \epsilon\left(\theta \epsilon_{\mathrm{min,p}} + (1-\theta)\epsilon_{\mathrm{min},K}\right) = 0.$$

- The factor θ which satisfies this relationship is then used to limit the entire solution $\mathbf{U_q}$ toward $\mathbf{U}_K$.

AMReX + `thornado`

- DG method is powerful, but problems are still computationally intensive.
- Including adaptive mesh refinement (AMR) through AMReX gives us high resolution only where needed[6].
- AMReX provides a parallel computing backend[6].
- AMR integration still in development, but parallel capabilities now used for many tests.

Characteristic Limiting Results

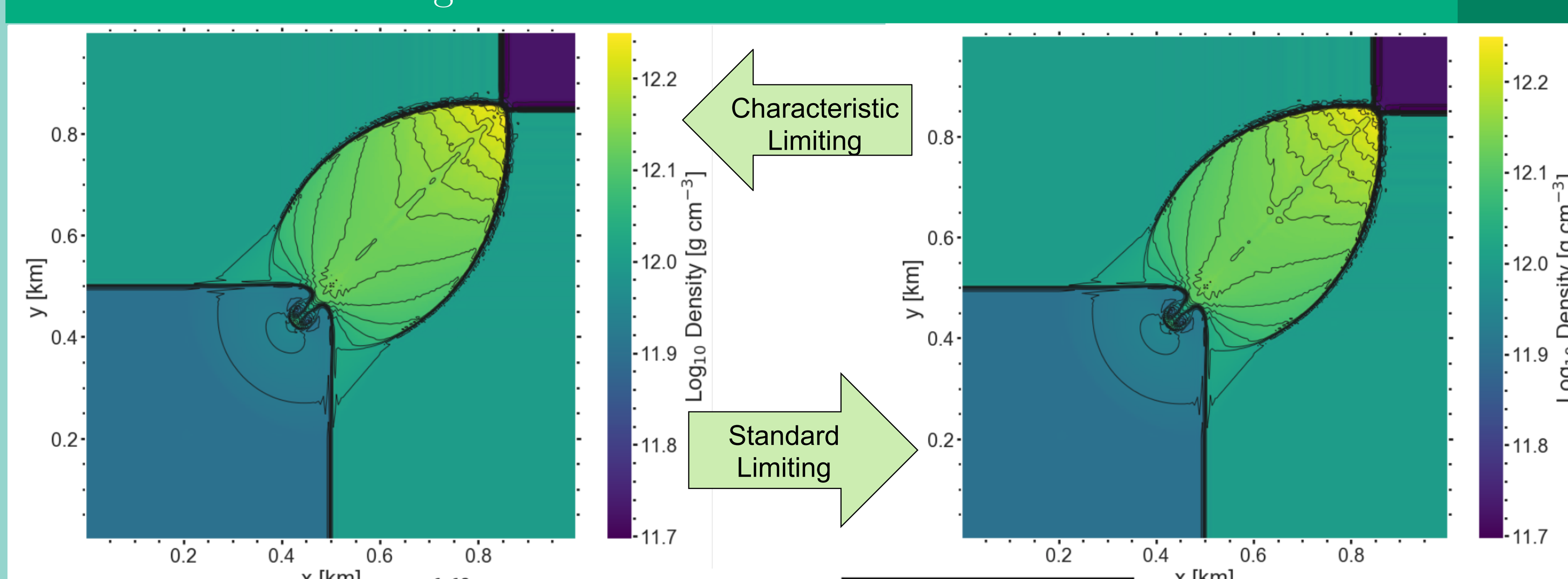

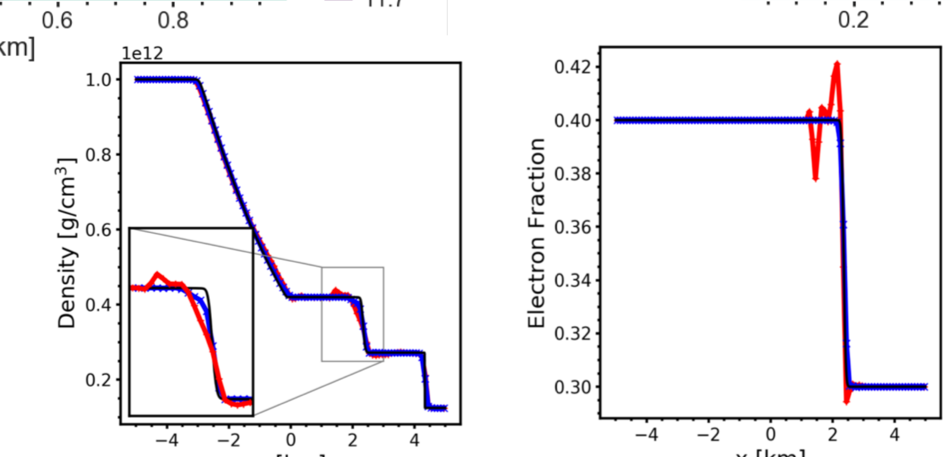

(Above) 2D density field for tests with characteristic (left) and standard (componentwise; right) limiting.

(Bottom) Density and electron fraction for Sod-like tests with characteristic (blue) and standard (red) limiting.

Positivity Limiting Results

- Left ($\boldsymbol{L}$) and right ($\boldsymbol{R}$) initial conditions for the 1D Sod shock tube for -5 km $< x < 5$ km:

$$\boldsymbol{L} = \{\rho = 1.25{\times}10^{15}\mathrm{g\ cm^{-3}}, v = 0\ \mathrm{km\ s^{-1}}, P = 6.35{\times}10^{35}\ \mathrm{erg\ cm^{-3}}, Y_e = 0.3\}$$
$$\boldsymbol{R} = \{\rho = 1.25{\times}10^{14}\mathrm{g\ cm^{-3}}, v = 0\ \mathrm{km\ s^{-1}}, P = 4.50{\times}10^{35}\mathrm{erg\ cm^{-3}}, Y_e = 0.3\}$$

- We currently enforce physicality at the minimum boundary.
- Figure (a) demonstrates the quadrature point solution for specific internal energy ϵ_q just above the EoS surface. Plotted over x, this solution remains above minimum boundary, see figure (b).
- Our solution resembles the profile of the reference solution for density, see figure (c).

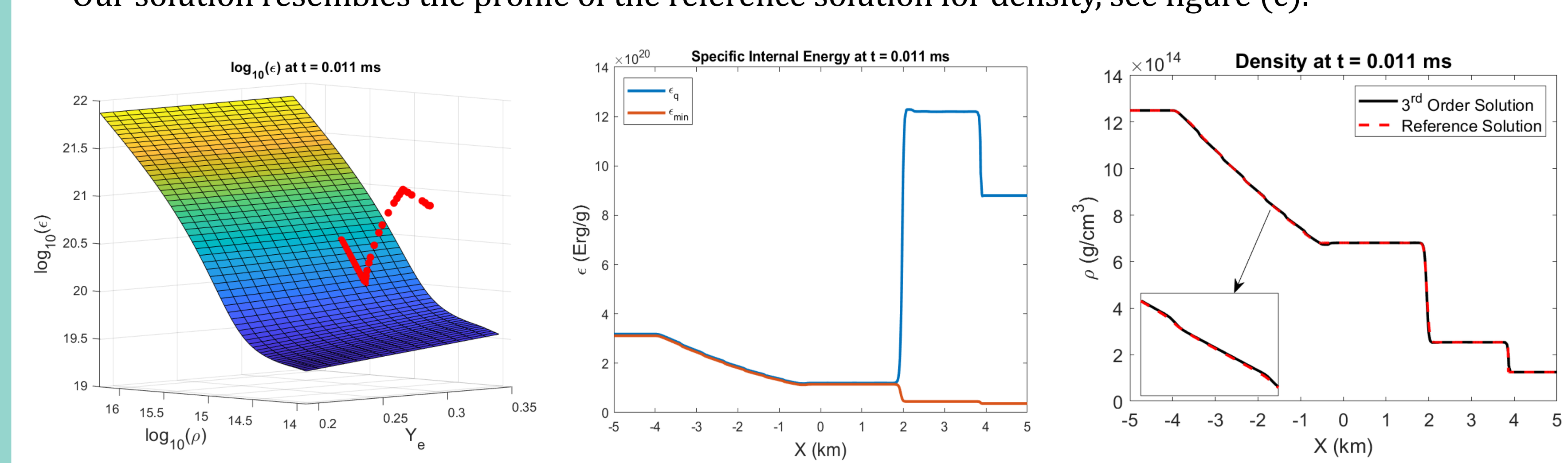

(a) $\log_{10}(\epsilon_q)$ plotted over DD2 nuclear EoS surface. (b) ϵ_q, as a function of x, plotted over the minimum table values of ϵ. (c) ρ_q plotted against a 1st order reference solution of 10,000 elements.

Current/Future Directions

- Enforce physicality at maximum boundary for nuclear EoS.
- Combine curvilinear coordinate and nuclear EoS capabilities.
- Explore modal decomposition and stability of the shock radius in the SAS problem.
- Continue integration with AMReX framework.
- Capabilities for relativistic hydrodynamics and neutrino transport concurrently in development.

Acknowledgements

We would like to thank the Department of Physics and Astronomy at The University of Tennessee, Knoxville, along with the Joint Institute for Computational Sciences.

This work was supported in part by the NSF Gravitational Physics Program (NSF-GP 1505933 and 1806692).

References

1. Hix, W. R. et al. *AIP Advances*, 4, 041013 (2014)
2. Zhang, X., and Shu, C.-W. *JCP*, vol. 229, no. 23, (2010), pp. 8918–8934
3. Endeve, E. et al. *J. Phy.: Conf. Ser.*, vol. 1225, 012014, (2019)
4. Blondin, J. et al. *ApJ*, vol. 584, (2003), pp. 971-980
5. Turk, M. et al. *ApJS*, vol. 192, (2011), pp. 9
6. Zhang, W. et al. *JOSS*, vol. 4, no. 37, (2019), pp.1370
7. Barker, B. et al. *UTK Chancellor's Honors Program Projects*, (2019)